

Machine Learning-Enhanced Feasibility Studies on the Production of New Particles with Preferential Couplings to Third Generation Fermions at the LHC

PhD(c). Cristian Fernando Rodríguez Cruz¹
c.rodriguez45@uniandes.edu.co

Research advisors:

Prof. Andrés Florez¹ (ca.florez@uniandes.edu.co)

Prof. J. Jones-Pérez² (jones.j@pucp.edu.pe)

¹Universidad de los Andes

²Pontificia Universidad Católica del Perú

January 21, 2026

Outline

1 Introduction

- Standard Model of Particle Physics
- Deficiencies of the SM
- LHC and Beyond the SM Physics

2 Phenomenological Framework

- Monte-Carlo Pipeline
- Hypothesis Testing & Statistical Significance
- Machine Learning in High Energy Physics

3 $U(1)_{T_R^3}$ Model

- Production Channel
- Search Channel
- Kinematic Variables
- Gradient Boosting

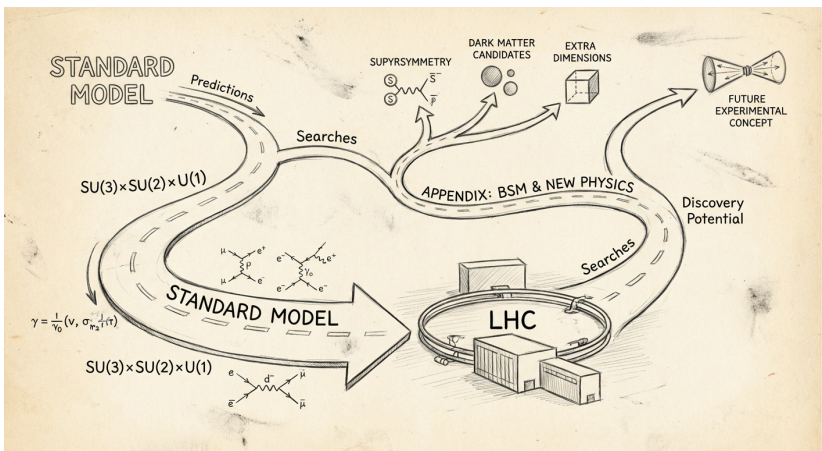
4 U_1 Leptoquark Model

- Kinematic Feature Eng.
- Single Channels Sensitivity Reach
- Combined Sensitivity Reach

5 Z' Interferences

6 Summary and Conclusions

Introduction



Standard Model of Particle Physics: A Successful Framework

Core Theoretical Structure

• Fermion Sector:

- 3 generations
- Left-handed doublets:

$$Q_L = \begin{pmatrix} q_u \\ q_d \end{pmatrix}_L ; \quad L_L = \begin{pmatrix} \ell \\ \nu_\ell \end{pmatrix}_L$$

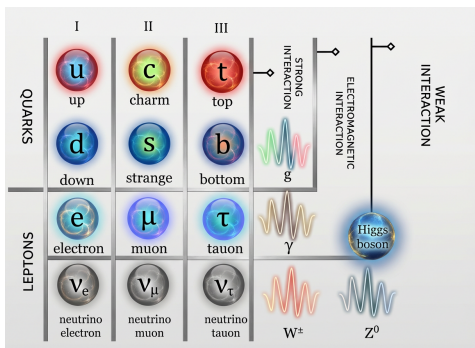
- Right-handed singlets: q_{uR}, q_{dR}, ℓ_R
- Flavor structure from CKM mixing
- Initially, ν_R not required (no mass)

• Gauge Group:

- $SU(3)_C \times SU(2)_L \times U(1)_Y$
- Strong force: $SU(3)_C$ (QCD)
- Electroweak: $SU(2)_L \times U(1)_Y$

• Higgs Mechanism:

- $SU(2)_L \times U(1)_Y \rightarrow U(1)_{EM}$
- Masses to W^\pm, Z^0 bosons
- Massless γ
- Fermion masses via Yukawa couplings
- Higgs boson h discovered (LHC 2012)



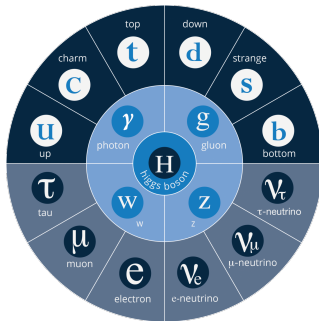
Key Features

- **Particle spectrum:** 12 fermions + 5 bosons
- **QFT:** Renormalizable, gauge invariant, anomaly-free
- **Tested experimentally:** Exceptional agreement with data
- **Predictive power:** Successfully tested at LHC

Deficiencies of the SM

The SM cannot be complete:

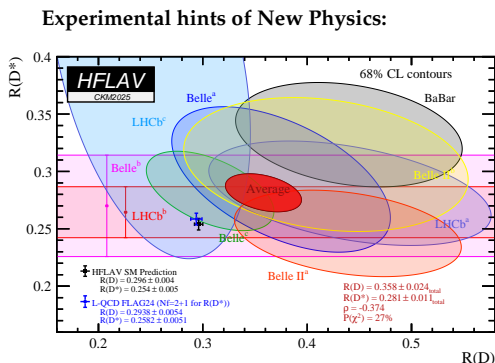
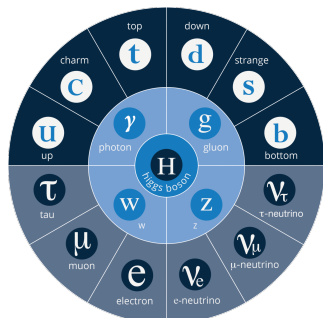
- Unexplained ν masses
- No explanation for DM
- Matter-antimatter asymmetry unsolved
- Gravity not included



Deficiencies of the SM

The SM cannot be complete:

- Unexplained ν masses
- No explanation for DM
- Matter-antimatter asymmetry unsolved
- Gravity not included



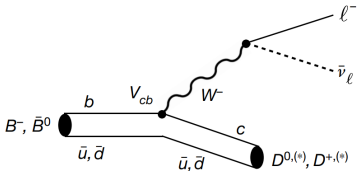
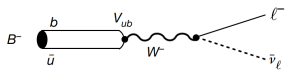
Recent measurements of the $R(D)$ and $R(D^*)$ ratios show a $\sim 3\sigma$ deviation from SM predictions, suggesting possible lepton universality violation.

$R(D)$ and $R(D^*)$ anomalies

Flavor Observables

$$R(D) = \frac{\text{BR}(B \rightarrow D \tau \nu)}{\text{BR}(B \rightarrow D \ell_{(e,\mu)} \nu)}, \quad R(D^{(*)}) = \frac{\text{BR}(B \rightarrow D^{(*)} \tau \nu)}{\text{BR}(B \rightarrow D^{(*)} \ell_{(e,\mu)} \nu)}$$

Standard Model (Tree-level)



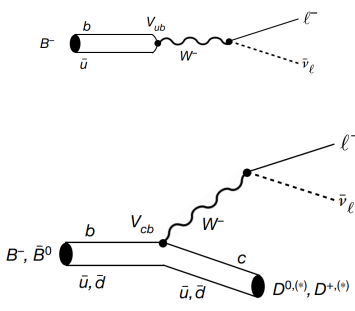
$B^- \rightarrow D^0 \ell^- \bar{\nu}_\ell$ via W^- exchange

$R(D)$ and $R(D^*)$ anomalies

Flavor Observables

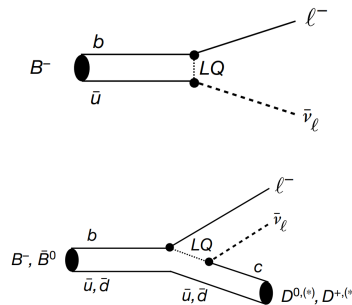
$$R(D) = \frac{\text{BR}(B \rightarrow D \tau \nu)}{\text{BR}(B \rightarrow D \ell_{(\epsilon, \mu)} \nu)}, \quad R(D^{(*)}) = \frac{\text{BR}(B \rightarrow D^{(*)} \tau \nu)}{\text{BR}(B \rightarrow D^{(*)} \ell_{(\epsilon, \mu)} \nu)}$$

Standard Model (Tree-level)



$B^- \rightarrow D^0 \ell^- \bar{\nu}_\ell$ via W^- exchange

Leptoquark Mediated



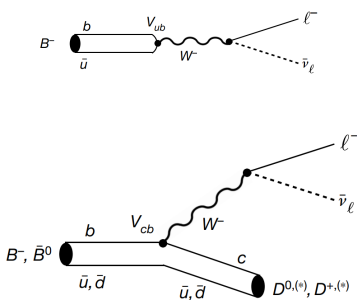
$B^- \rightarrow D^0 \ell^- \bar{\nu}_\ell$ via leptoquark exchange

$R(D)$ and $R(D^*)$ anomalies

Flavor Observables

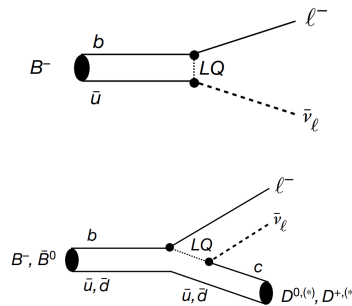
$$R(D) = \frac{\text{BR}(B \rightarrow D \tau \nu)}{\text{BR}(B \rightarrow D \ell_{(\epsilon, \mu)} \nu)}, \quad R(D^{(*)}) = \frac{\text{BR}(B \rightarrow D^{(*)} \tau \nu)}{\text{BR}(B \rightarrow D^{(*)} \ell_{(\epsilon, \mu)} \nu)}$$

Standard Model (Tree-level)



$B^- \rightarrow D^0 \ell^- \bar{\nu}_\ell$ via W^- exchange

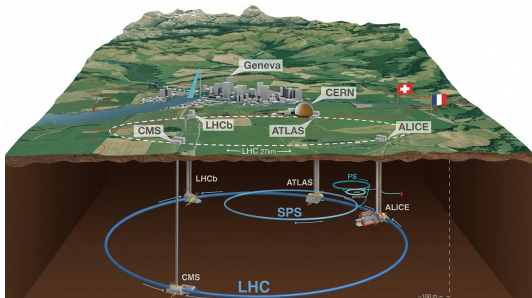
Leptoquark Mediated



$B^- \rightarrow D^0 \ell^- \bar{\nu}_\ell$ via leptoquark exchange

How can we test this hypothesis?

The Large Hadron Collider (LHC)

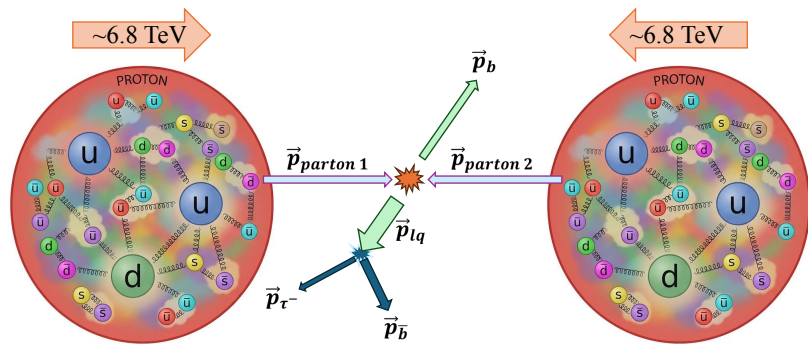


World's largest particle collider:

- Located at CERN, at the France-Switzerland border
- 27 km circumference ring
- Currently running proton-proton collisions at $\sqrt{s} = 13.6$ TeV
- Designed to probe the TeV scale
- Four main experiments: ATLAS, CMS, LHCb, ALICE
- High luminosity upgrade (HL-LHC) planned for 2029
- Key tool for testing SM and exploring new physics scenarios
- Now searching for physics **beyond the Standard Model**

The Quark-Gluon Sea

Partons are the fundamental constituents inside protons: valence quarks (uud) and a **sea** of virtual quark-antiquark pairs and gluons.

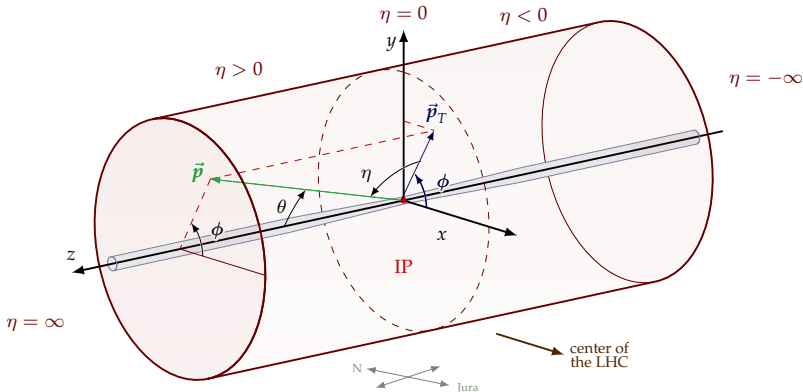


The interacting partons are typically **sea quarks or gluons**, which carry only a fraction of the proton's momentum but dominate the cross-section at high energies.

Kinematic Variables

From Spherical coordinates,

$$\left\{ \begin{array}{l} \text{Pseudorapidity: } \eta = -\ln \tan(\theta/2) \\ \text{Transverse momentum: } p_T = p \sin(\theta) \\ \text{Azimuthal angle: } \phi \\ \text{Deposited energy: } E \end{array} \right.$$

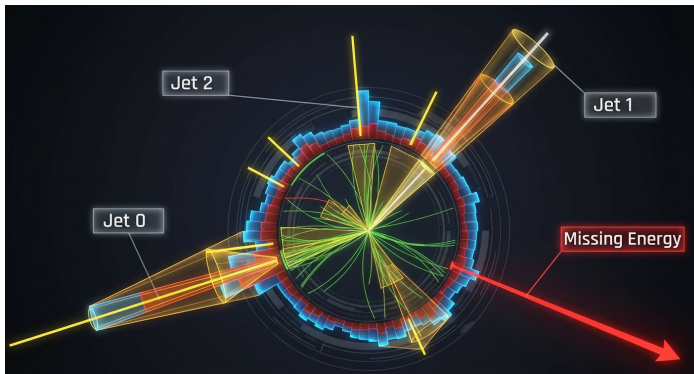


Jet Clustering & Missing Transverse Momentum

Jet clustering groups collimated particle showers into jets to reconstruct the original quarks/gluons from the hard scatter.

Missing p_T appears as transverse momentum imbalance, signaling undetected particles like neutrinos:

$$\vec{p}_T^{\text{miss}} = - \sum_{\text{visible prods}} \vec{p}_T$$



What Do We Look For at the LHC?

Three Complementary Approaches

• SM Parameter Determination

- Precisely measure fundamental SM parameters
- Test consistency of the SM framework
- Reduce theoretical uncertainties

• Indirect Searches (Precision Tests)

- Measure SM processes with high precision
- Look for deviations in predicted distributions
- Constrain new physics through virtual effects

• Direct Searches

- Look for new particles in final states (resonances, excesses)
- Examples: SUSY particles, Z' , leptoquarks, dark matter mediators

Key Types of Measurements

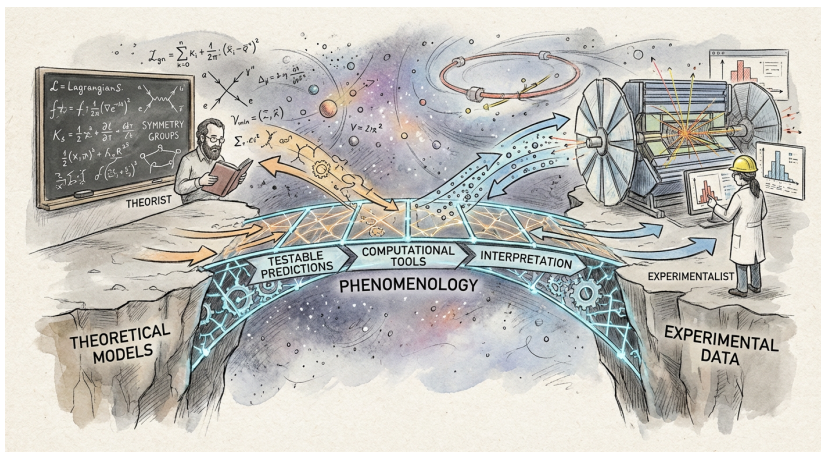
Direct Signatures:

- Resonant mass peaks
- Excess events over SM background
- Missing transverse energy (MET)
- Unusual kinematic features

Precision Observables:

- Differential cross sections
- Angular correlations
- Rare decay rates
- Lepton flavor universality ratios
- Charge-parity (CP) asymmetries

Phenomenological Framework



From Theory to Simulation: FeynRules



Input: .fr Model File

- Lagrangian \mathcal{L} terms
- Particle definitions: F, V, S fields
- Gauge symmetries: $SU(N)$, $U(1)$
- Parameters: masses, couplings
- Mixing matrices, constraints

Output: UFO Format

- Complete Feynman rules (vertices)
- Lorentz and color structures
- Parameter definitions
- Ready to simulate

Features

- ↗ Standardized UFO format
- ↗ Flexible for BSM models
- ↗ Community-driven
- ↘ NLO complexity
- ↘ Poor debugging
- ↘ Performance issues

Why Simulate New Physics Models?

- **Predict signals** for experimental searches
- **Test theoretical consistency** (unitarity, constraints)
- **Optimize analyses** before data collection
- **Interpret potential discoveries** from LHC data
- **Compare predictions** across different models

Madgraph-Pythia-Delphes

Ecosystem for Event Simulation

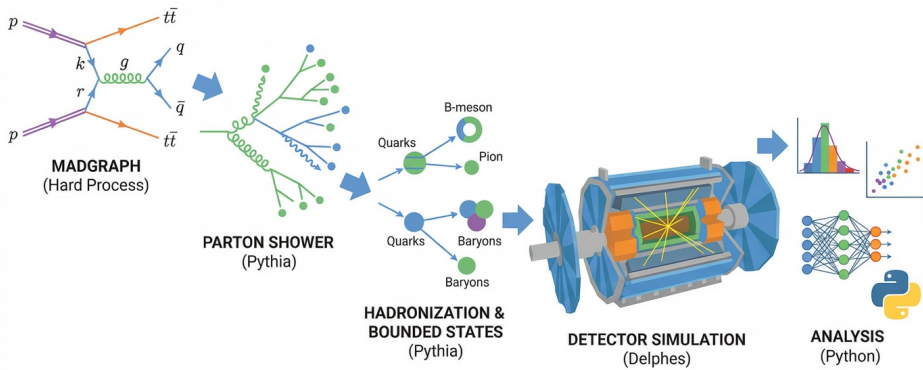
Goal: Produce realistic simulated data comparable to experimental observations

Input: BSM model in UFO format, collider setup, process definitions, parameters

Pipeline: UFO model → LHE (parton) → HEPMC (hadron) → ROOT (detector)

Output: Simulated events in ROOT format, ready for physics analysis

Automated: Cross-sections, widths, branching ratios calculated automatically



Statistical Significance

The statistical significance for discovery is a parametric test defined as:

$$\kappa = \frac{\langle t \rangle_B - \langle t \rangle_{S+B}}{\sigma_{S+B}} \quad (1)$$

where $t = -2 \ln[\mathcal{L}(n|S + B)/\mathcal{L}(n|B)] \sim \chi^2$ is the optimal test statistic.

We denote \mathcal{L} as the likelihood for Poisson-distributed event counts n in each bin and gaussian systematic uncertainties.

For binned data analysis, this simplifies to:

$$\kappa = \frac{\sum_i s_i w_i}{\sqrt{\sum_i (s_i + b_i + \delta_{\text{sys}}^2) w_i^2}} \quad (2)$$

where s_i, b_i are signal/background events in bin i , $w_i \sim \ln(1 + s_i/b_i)$ are optimal weights, and δ_{sys} is the systematic uncertainty.

Exclusion criterion: A hypothesis with $\kappa \leq 1.69\sigma$ can be excluded at 95% CL.

Optimizing Sensitivity

The event yield in each bin is $N_i = \sigma_i \cdot \mathcal{L} \cdot \epsilon_i$, where:

- σ_i : cross section
- \mathcal{L} : integrated luminosity
- ϵ_i : selection efficiency

The significance becomes:

$$\kappa = \frac{\sum_i \sigma_{s_i} \epsilon_{s_i} w_i}{\sqrt{\sum_i (\sigma_{s_i} \epsilon_{s_i} + \sigma_{b_i} \epsilon_{b_i} + \delta_{\text{sys}}^2) w_i^2}} \sqrt{\mathcal{L}} \quad (3)$$

Strategies to improve κ :

- Increase luminosity \mathcal{L}
- Optimize cuts to enhance ϵ_s/ϵ_b
- Increase σ_s via higher \sqrt{s} for heavier states
- Use multivariate discriminants (BDT, DNN)
- Reduce systematic uncertainties δ_{sys}
- Exploit correlations between bins

Machine Learning Revolution in HEP

Why ML in Particle Physics?

- **High-dimensional data:**
Complex detector outputs
- **Complex patterns:**
Jet and event classification
- **Rare signals:**
Need optimal background rejection
- **Automation:**
Reduce manual feature engineering
- **Computational efficiency:**
Speed up workflows

Traditional vs ML Approaches

Traditional:

- Manual cut-based analysis
- Simple kinematic variables
- Likelihood methods

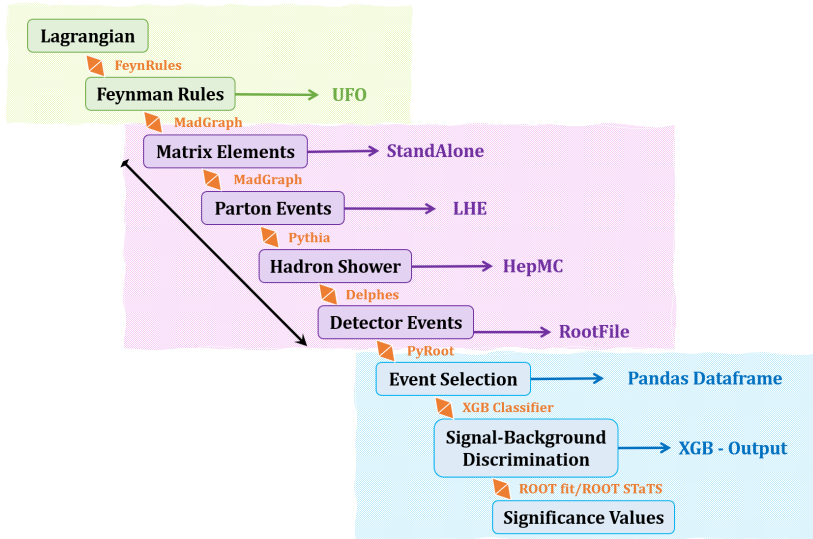
Machine Learning:

- Multivariate classifiers (BDT, NN)
- Deep learning on raw data
- Anomaly detection for BSM searches

Typical Current Applications

- **Event classification:** Signal/background separation
- **Jet tagging:** $b/c/\tau$ -jet identification
- **Object reconstruction:** Particle flow, tracking
- **Anomaly detection:** Model-agnostic BSM searches
- **Simulation acceleration:** Fast calorimeter simulation

Feasibility Studies Workflow



$U(1)_{T_R^3}$ Model

To do ADD production channel diagrams

Feasible Experimental Signatures

Cross Section

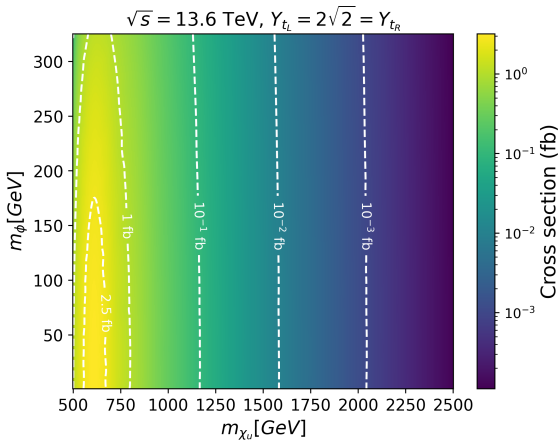
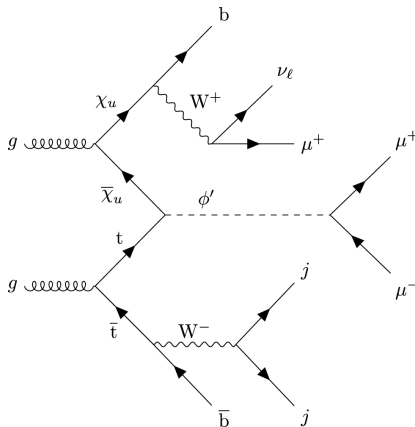


Fig.: Projected cross section (fb) plot for $pp \rightarrow t\chi_u \phi'$ and subsequent decay as a function of $m(\chi_u)$ and $m(\phi')$.

Feasible Experimental Signatures

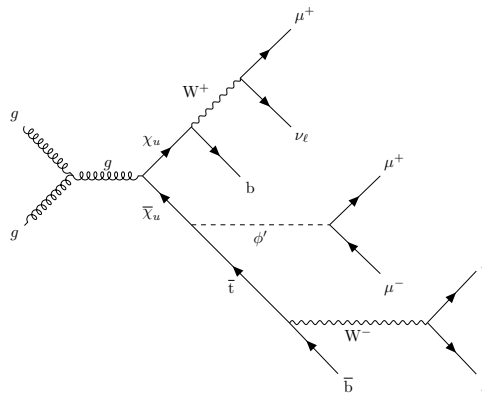
Representative Feynman diagram for the production of a ϕ' boson in association with a χ_u vector-like quark through the fusion of a top quark and χ_u vector-like quark.



The ϕ' decays to a pair of muons, the top quark decays fully hadronically, and the χ_u decays semi-leptonically to muons, neutrinos and b -jets.

Feasible Experimental Signatures

Representative Feynman diagram for the production of a ϕ' boson in association with a χ_u vector-like quark through the fusion of a gluon pair from incoming protons.

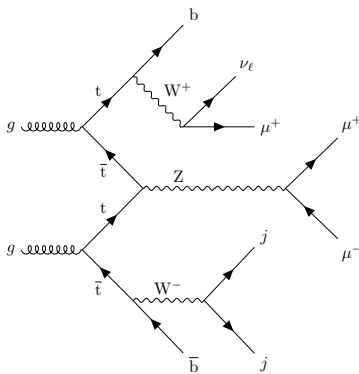


The ϕ' decays to a pair of muons, the top quark that decays fully hadronically, and the χ_u decay semi-leptonically to muons, neutrinos and jets.

Feasible Experimental Signatures

Background

Representative Feynman diagram for a background event. A Z boson is produced in association with a top quark through the fusion of a top, anti top pair from incoming protons.



The Z boson subsequently decays to a pair of muons and the two spectator top quarks decay semi-leptonically and purely hadronically to muons, neutrinos and jets, resulting in the same final states as the signal event.

Feasible Experimental Signatures

Kinematic Variables

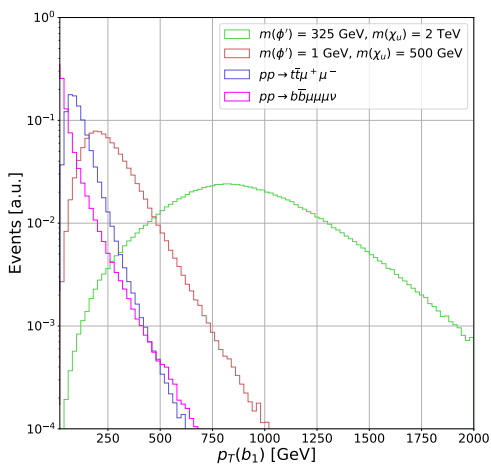


Fig.: Transverse momentum distribution of the leading b-quark jet candidate. The distributions are shown for the two main SM background processes and two signal benchmark points.

Feasible Experimental Signatures

Kinematic Variables

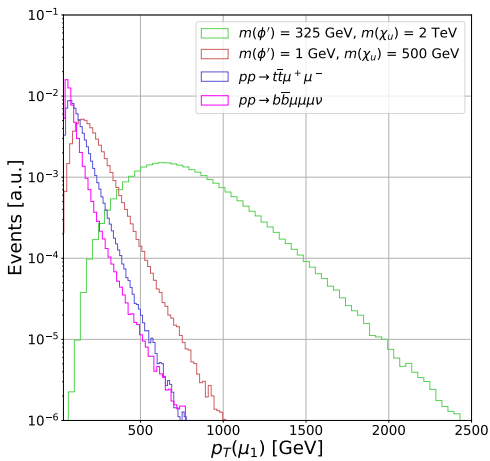


Fig.: Transverse momentum distribution of the leading muon candidate. The distributions are shown for the two main SM background processes and two signal benchmark points.

Feasible Experimental Signatures

Kinematic Variables

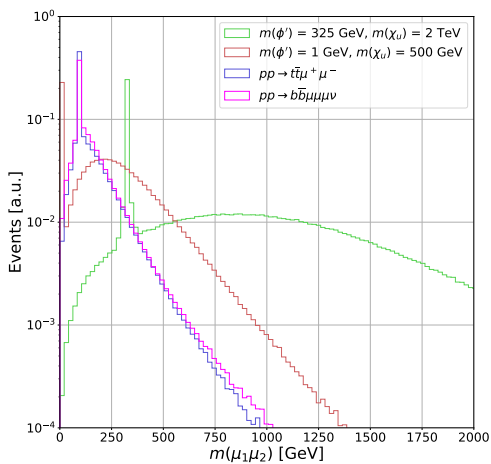


Fig.: Invariant mass distribution of the muon pair with the highest and second highest transverse momentum. The distributions are shown for the two main SM background processes and two signal benchmark points.

Gradient Boosting

Feasible Experimental Signatures

Gradient Boosting

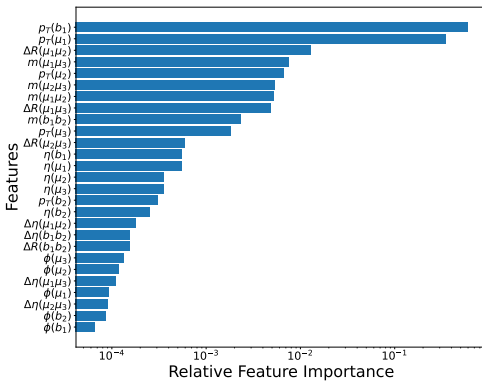


Fig.: Relative importance of features in training for a benchmark signal scenario with $m(\phi') = 325 \text{ GeV}$ and $m(\chi_u) = 2000 \text{ GeV}$.

Feasible Experimental Signatures

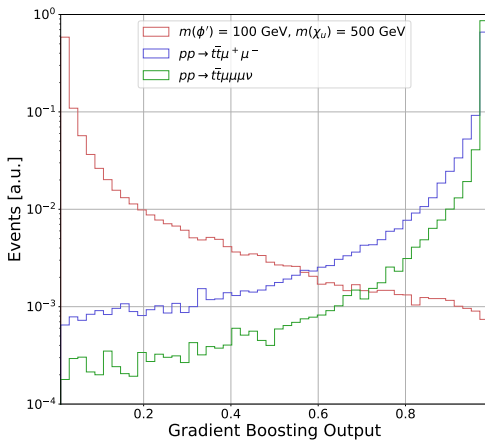


Fig.: Output of the gradient boosting algorithm for a benchmark $m(\phi') = 100$ GeV and $m(\chi_u) = 500$ GeV signal, and dominant backgrounds. The distributions are normalized to unity.

Signal Significance

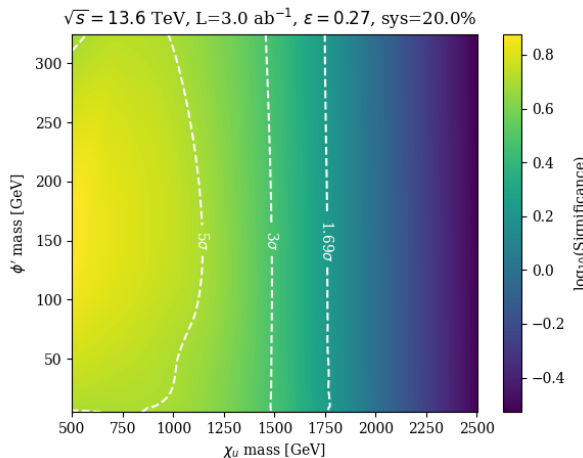


Fig.: Signal significance for the high luminosity LHC era, considering with 3000 fb^{-1} of collected data.

U_1 Leptoquark Model

The vector leptoquark U_1 model

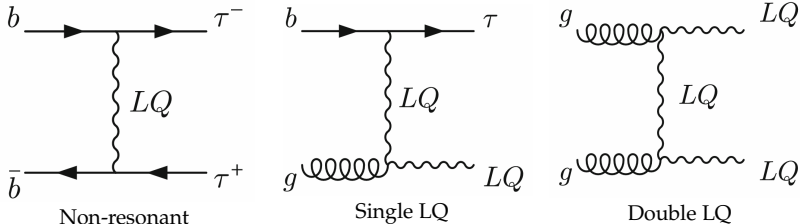
A leptoquark is defined as a particle with a vertex that mix vectors and quarks.

If U_1 is a vector leptoquark that preserves the chirality on the vertex, we expect an interaction term like

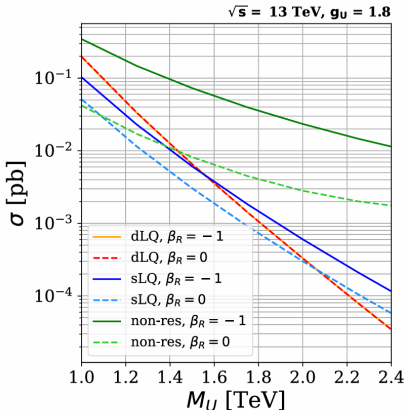
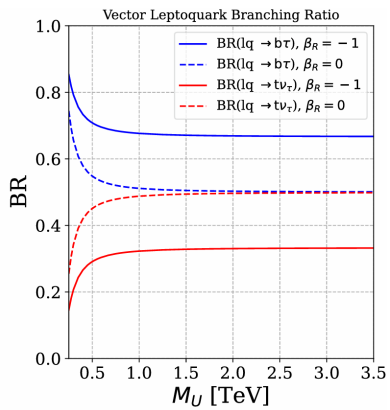
$$\sim \beta_L U_1^\mu \bar{q}_L \gamma_\mu \ell_L,$$

and these allows a similar interaction term for the right handed currents

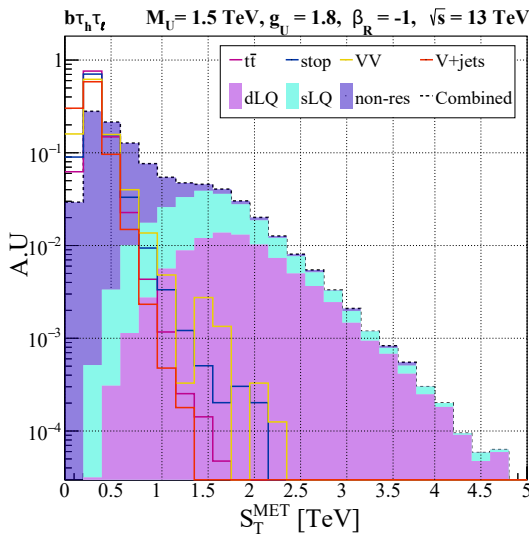
$$\sim \beta_R U_1^\mu \bar{d}_R \gamma_\mu e_R.$$



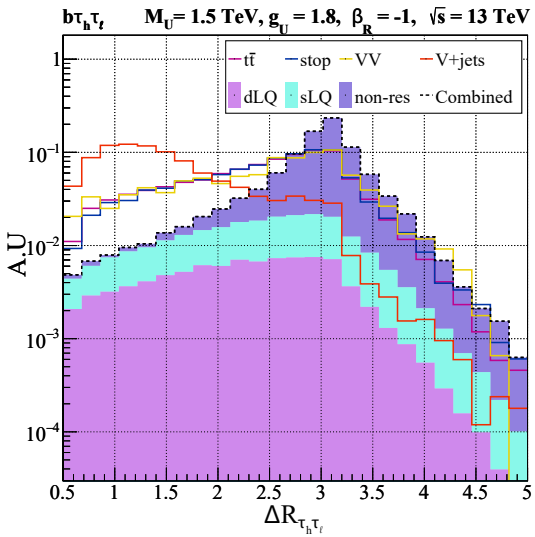
Leptoquark Production at pp Colliders



$$S_T^{\text{met}} = \text{met} + \sum_i |p_T^i|$$



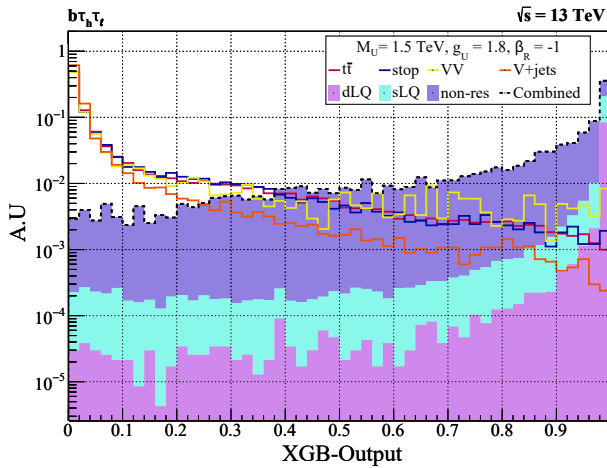
$$\Delta R = \sqrt{\Delta\eta^2 + \Delta\phi^2}$$



The optimized observable

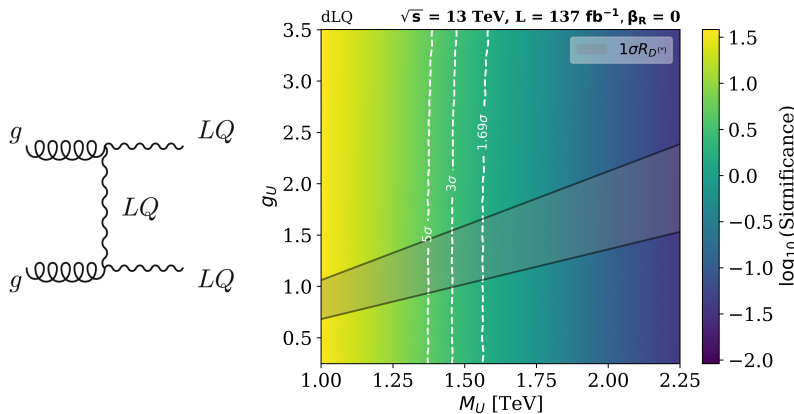
XGB-output

We can evaluate a score for the signal and background events using the discriminator algorithm.



Double Leptoquark Production

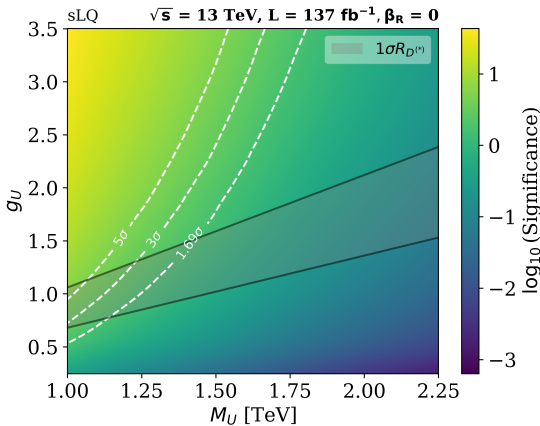
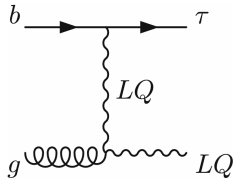
The Sensitivity Reach / only left-handed currents



Double leptoquark production is sensitive to the leptoquark mass, its production depends only on the QCD coupling constant and the available energy.

Single leptoquark production

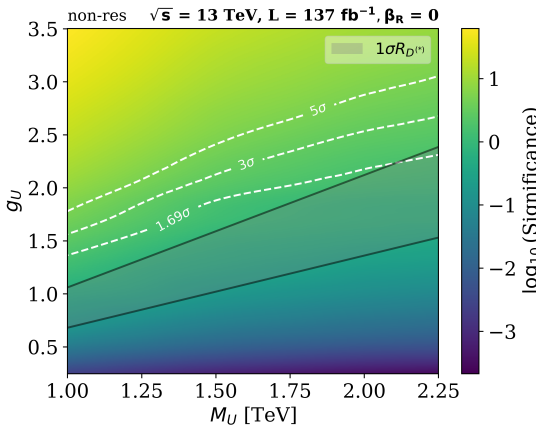
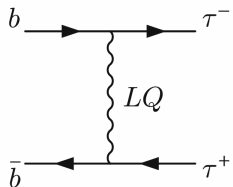
The Sensitivity Reach / only left-handed currents



Single leptoquark production is sensitive to both, mass and couplings. It contributes to the regions of high coupling constants at higher masses than double leptoquark production.

Non-resonant Production

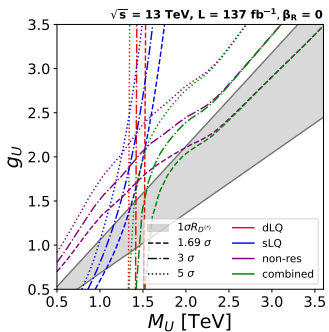
The Sensitivity Reach / only left-handed currents



Non-resonant production is highly dependent on the couplings, so it dominates the regions of high coupling constants at all masses.

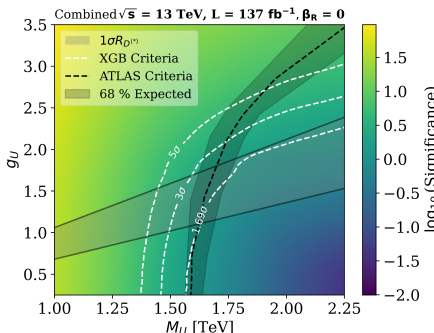
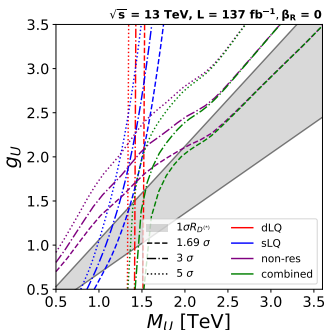
Combined Sensitivity Reach

The Sensitivity Reach / only left-handed currents



Combined Sensitivity Reach

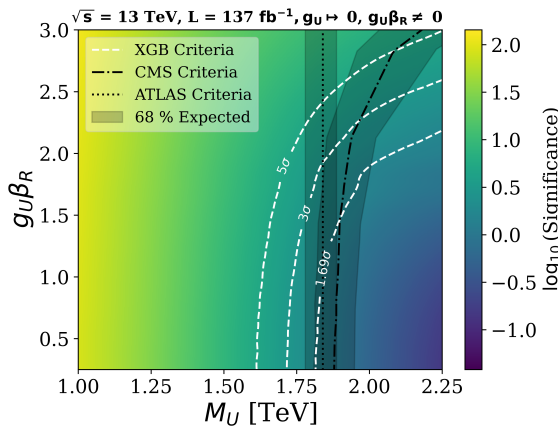
The Sensitivity Reach / only left-handed currents



The sensitivity of all signal production processes combined compares our expected exclusion region with the latest one from the ATLAS Collaboration [ArXiv:2305.15962], but we suggest better sensitivity for high coupling constants.

Combined Sensitivity Reach

The Sensitivity Reach / only right-handed currents



The case $BR(lq \rightarrow b\tau) = 1$ corresponds to the only right-handed currents coupling. The sensitivity compared with the latest one from the CMS [2308.07826] and ATLAS Collaborations [2303.01294], again we suggest better sensitivity for high coupling constants.

Z' Interferences

The need of a Z' boson in gauge U_1 models

If U_1 has a gauge origin, we could rewrite the interaction term in the covariant derivative as

$$\psi_L^{\text{SM}} = \begin{pmatrix} q_{Lr} \\ q_{Lg} \\ q_{Lb} \\ \ell_L \end{pmatrix} \implies \mathcal{L}_{\text{int}} \sim U_{1\alpha}^\mu \bar{\psi}_L^{\text{SM}} \gamma_\mu T_+^\alpha \psi_L^{\text{SM}} + \text{h.c.}, \quad T_+^\alpha = \begin{pmatrix} 0 & 0 & 0 & \delta_{r\alpha} \\ 0 & 0 & 0 & \delta_{g\alpha} \\ 0 & 0 & 0 & \delta_{b\alpha} \\ 0 & 0 & 0 & 0 \end{pmatrix},$$

we have six generators T_\pm^α with closure relation and projecting into a color singlet operator:

$$\sum_\alpha [T_+^\alpha, T_-^\alpha] = 3T_{B-L} = \begin{pmatrix} 1 & 0 & 0 & 0 \\ 0 & 1 & 0 & 0 \\ 0 & 0 & 1 & 0 \\ 0 & 0 & 0 & -3 \end{pmatrix}.$$

So, the gauge group with this leptoquark must include a $U(1)_{B-L}$ symmetry (The right-handed currents also have a similar interaction term).

The need of a Z' boson in gauge U_1 models

If U_1 has a gauge origin, we could rewrite the interaction term in the covariant derivative as

$$\psi_L^{\text{SM}} = \begin{pmatrix} q_{Lr} \\ q_{Lg} \\ q_{Lb} \\ \ell_L \end{pmatrix} \implies \mathcal{L}_{\text{int}} \sim U_{1\alpha}^\mu \bar{\psi}_L^{\text{SM}} \gamma_\mu T_+^\alpha \psi_L^{\text{SM}} + \text{h.c.}, \quad T_+^\alpha = \begin{pmatrix} 0 & 0 & 0 & \delta_{r\alpha} \\ 0 & 0 & 0 & \delta_{g\alpha} \\ 0 & 0 & 0 & \delta_{b\alpha} \\ 0 & 0 & 0 & 0 \end{pmatrix},$$

we have six generators T_\pm^α with closure relation and projecting into a color singlet operator:

$$\sum_\alpha [T_+^\alpha, T_-^\alpha] = 3T_{B-L} = \begin{pmatrix} 1 & 0 & 0 & 0 \\ 0 & 1 & 0 & 0 \\ 0 & 0 & 1 & 0 \\ 0 & 0 & 0 & -3 \end{pmatrix}.$$

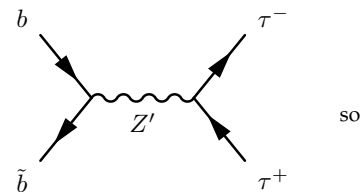
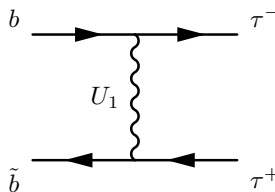
So, the gauge group with this leptoquark must include a $U(1)_{B-L}$ symmetry (The right-handed currents also have a similar interaction term).

The interaction terms for the Z' boson have the form

$$\begin{aligned} \mathcal{L}_{\text{int}} &\sim Z'_\mu \left(\bar{\psi}_L^{\text{SM}} \gamma^\mu (3T_{B-L}) \psi_L^{\text{SM}} \right) \\ &\sim Z'_\mu \left(\bar{q}_L \gamma^\mu q_L - 3\bar{\ell}_L \gamma^\mu \ell_L \right). \end{aligned}$$

Interference with a Z' vector boson

Non-Resonant Production (leptoquarks) Resonant Production (neutral bosons)



so

$$\mathcal{M}_{U_1} \sim \frac{1}{t - m_{U_1}^2 + im_{U_1}\Gamma_{U_1}}, \quad (4)$$

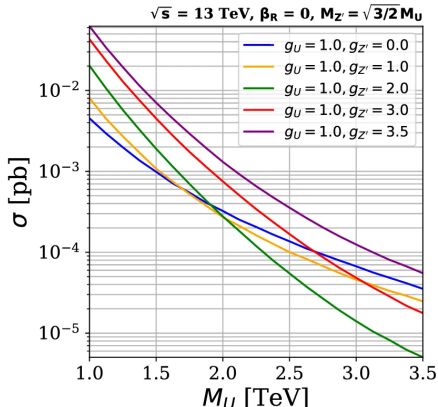
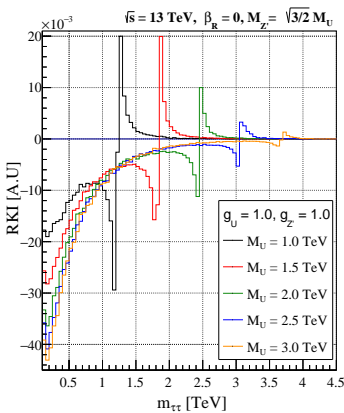
$$\mathcal{M}_{Z'} \sim \frac{1}{s - m_{Z'}^2 + im_{Z'}\Gamma_{Z'}}, \quad (5)$$

the interference has the form

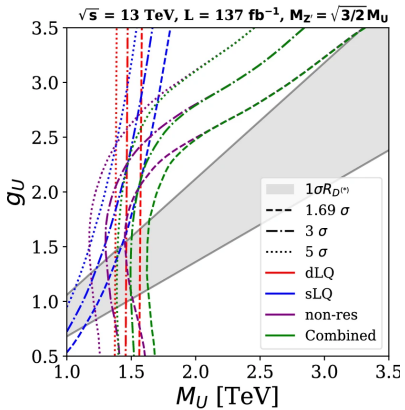
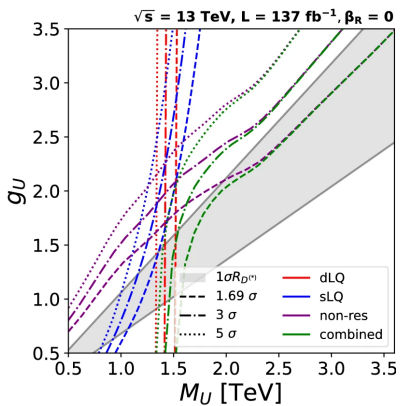
$$\frac{d}{dm} \left[\sigma_{LQ+Z'} - \left(\sigma_{LQ} + \sigma_{Z'} \right) \right] \sim \frac{g_{z'} g_U}{s} \frac{m_{LQ} m_{Z'} \Gamma_{LQ} \Gamma_{Z'} - (t - m_{LQ}^2)(s - m_{Z'}^2)}{\left[(t - m_{LQ}^2)^2 + m_{LQ}^2 \Gamma_{LQ}^2 \right] \left[(s - m_{Z'}^2)^2 + m_{Z'}^2 \Gamma_{Z'}^2 \right]}.$$

Similary for Polarized final states.

Interference with a Z' vector boson



Effects on the Sensitivity reach



Summary and Conclusions

Backup Slides

Where the SM charges for the leptoquark, in the $Y = 2(Q - T_3)$ convention, are

	\bar{q}_L	ℓ_L^j	$\bar{q}_L \gamma_\mu \ell_L$	U_1^μ
$U(1)$	$-1/3$	-1	$-4/3$	$+4/3$
$SU(2)$	$\bar{\mathbf{2}}$	$\mathbf{2}$	$\mathbf{1}$	$\mathbf{1}$
$SU(3)$	$\bar{\mathbf{3}}$	$\mathbf{1}$	$\mathbf{3}$	$\mathbf{3}$

Then, the leptoquark $U_1 \sim (\mathbf{3}_C, \mathbf{1}_I, 4/3_Y)$.

Where the SM charges for the leptoquark, in the $Y = 2(Q - T_3)$ convention, are

	\bar{q}_L	ℓ_L^j	$\bar{q}_L \gamma_\mu \ell_L$	U_1^μ
$U(1)$	$-1/3$	-1	$-4/3$	$+4/3$
$SU(2)$	$\bar{\mathbf{2}}$	$\mathbf{2}$	$\mathbf{1}$	$\mathbf{1}$
$SU(3)$	$\bar{\mathbf{3}}$	$\mathbf{1}$	$\mathbf{3}$	$\mathbf{3}$

Then, the leptoquark $U_1 \sim (\mathbf{3}_C, \mathbf{1}_I, 4/3_Y)$.

The full Lagrangian for the vector leptoquark is

$$\begin{aligned} \mathcal{L}_U = & -\frac{1}{2} U_{\mu\nu}^\dagger U^{\mu\nu} + M_U^2 U_\mu^\dagger U^\mu - i g_s U_\mu^\dagger T^a U_\nu G_a^{\mu\nu} - \frac{2i}{3} g' U_\mu^\dagger U_\nu B^{\mu\nu} \\ & + \frac{g_u}{\sqrt{2}} \left[U_1^\mu \left(\beta_L^{ij} \bar{q}_L^i \gamma_\mu e_L^j + \beta_R^{ij} \bar{d}_R^i \gamma_\mu e_R^j \right) + \text{h.c.} \right] \end{aligned}$$

where $U_{\mu\nu} = \mathcal{D}_\mu U_\nu - \mathcal{D}_\nu U_\mu$, $\mathcal{D}_\mu = \partial_\mu - i g_s G_\mu^a T^a - i \frac{2}{3} g_Y B_\mu$, and the couplings β_L and β_R are complex 3×3 matrices in flavor space.

Where the SM charges for the leptoquark, in the $Y = 2(Q - T_3)$ convention, are

	\bar{q}_L	ℓ_L^j	$\bar{q}_L \gamma_\mu \ell_L$	U_1^μ
$U(1)$	$-1/3$	-1	$-4/3$	$+4/3$
$SU(2)$	$\bar{\mathbf{2}}$	$\mathbf{2}$	$\mathbf{1}$	$\mathbf{1}$
$SU(3)$	$\bar{\mathbf{3}}$	$\mathbf{1}$	$\bar{\mathbf{3}}$	$\mathbf{3}$

Then, the leptoquark $U_1 \sim (\mathbf{3}_C, \mathbf{1}_I, 4/3_Y)$.

The full Lagrangian for the vector leptoquark is

$$\begin{aligned} \mathcal{L}_U = & -\frac{1}{2} U_{\mu\nu}^\dagger U^{\mu\nu} + M_U^2 U_\mu^\dagger U^\mu - i g_s U_\mu^\dagger T^a U_\nu G_a^{\mu\nu} - \frac{2i}{3} g' U_\mu^\dagger U_\nu B^{\mu\nu} \\ & + \frac{g_u}{\sqrt{2}} \left[U_1^\mu \left(\beta_L^{ij} \bar{q}_L^i \gamma_\mu e_L^j + \beta_R^{ij} \bar{d}_R^i \gamma_\mu e_R^j \right) + \text{h.c.} \right] \end{aligned}$$

where $U_{\mu\nu} = \mathcal{D}_\mu U_\nu - \mathcal{D}_\nu U_\mu$, $\mathcal{D}_\mu = \partial_\mu - i g_s G_\mu^a T^a - i \frac{2}{3} g_Y B_\mu$, and the couplings β_L and β_R are complex 3×3 matrices in flavor space.

Constraints from $\Delta F = 2$ and lepton flavor violation impose a hierarchy with dominant third generation couplings:

$$|\beta_L^{11}|, |\beta_L^{12}|, |\beta_L^{21}|, |\beta_L^{22}|, |\beta_L^{31}| \ll |\beta_L^{13}| \ll |\beta_L^{23}|, |\beta_L^{32}| \ll |\beta_R^{33}|, |\beta_L^{33}| = \mathcal{O}(1), \quad (6)$$

where β_R is diagonal.

Two body scattering

CM-Frame

Consider the process

$$A(\vec{p}_1) + B(\vec{p}_2) \longrightarrow C(\vec{p}_3) + D(\vec{p}_4), \quad (7)$$



From the Golden Rule, the cross section is given by

$$\sigma = \frac{n!(2\pi)^4}{4\sqrt{(\vec{p}_1 \cdot \vec{p}_2)^2 - (m_1 m_2)^2}} \int |\mathcal{M}|^2 \delta^{(4)}(p_1 + p_2 - p_3 - p_4) \frac{d^3 \vec{p}_3}{(2\pi)^3 2E_3} \frac{d^3 \vec{p}_4}{(2\pi)^3 2E_4}. \quad (8)$$

But, in the CM frame, $\vec{p}_1 + \vec{p}_2 = 0$, where

$$\sqrt{(\vec{p}_1 \cdot \vec{p}_2)^2 - (m_1 m_2)^2} = E_1 E_2 |\vec{p}_1|, \quad (9)$$

$$\delta^{(4)}(p_1 + p_2 - p_3 - p_4) = \delta(E_1 + E_2 - E_3 - E_4) \delta^{(3)}(\vec{p}_3 + \vec{p}_4). \quad (10)$$

Thus

$$\sigma = \left(\frac{1}{8\pi}\right)^2 \frac{n!}{(E_1 E_2) |\vec{p}_1|} \int |\mathcal{M}|^2 \frac{\delta(E_1 + E_2 - \sqrt{\vec{p}_3^2 + m_3^2} - \sqrt{\vec{p}_4^2 + m_4^2})}{\sqrt{\vec{p}_3^2 + m_3^2} \sqrt{\vec{p}_4^2 + m_4^2}} d\vec{p}_3 \quad (11)$$

Integrating over the radial part $|\vec{p}_3|$, we get

$$\sigma = \left(\frac{1}{8\pi}\right)^2 \frac{n! |\vec{p}_3|}{(E_1 + E_2)^2 |\vec{p}_1|} \int |\mathcal{M}|^2 d\Omega, \quad (12)$$

with

$$|\vec{p}_3| = \frac{1}{2} \frac{\sqrt{((E_1 + E_2)^2 - m_3^2 - m_4^2)^2 - 4m_3^2 m_4^2}}{E_1 + E_2}, \quad (13)$$

the outgoing momentum in the CM frame.

We prefer work with differential cross section as

$$\frac{d\sigma}{d\Omega} = \frac{1}{64\pi^2} \frac{n!}{(E_1 + E_2)^2} \frac{|\vec{p}_3|}{|\vec{p}_1|} |\mathcal{M}|^2. \quad (14)$$

Defining $\sqrt{s} = E_1 + E_2$, we have

$$|\vec{p}_3| = \frac{1}{2} \frac{\sqrt{(s - m_3^2 - m_4^2)^2 - 4m_3^2 m_4^2}}{\sqrt{s}}, \quad |\vec{p}_1| = \frac{1}{2} \frac{\sqrt{(s - m_1^2 - m_2^2)^2 - 4m_1^2 m_2^2}}{\sqrt{s}}. \quad (15)$$

so the differential cross section is

$$\frac{d\sigma}{d\Omega} = \frac{1}{64\pi^2} \frac{n!}{s} \sqrt{\frac{(s - (m_3 + m_4)^2)(s - (m_3 - m_4)^2)}{(s - (m_1 + m_2)^2)(s - (m_1 - m_2)^2)}} |\mathcal{M}|^2. \quad (16)$$

Note that at this point, we don't need to know the explicit form of the matrix element \mathcal{M} , so it is a generic result.

Writting t in terms of s and θ

In general, there are three Lorentz-invariant useful kinematical variables to describe the scattering process, known as Mandelstam variables:

$$\hat{s} = (p_1 + p_2)^2 = (p_3 + p_4)^2 = m_1^2 + m_2^2 + 2p_1^\mu p_{2\mu} = m_3^2 + m_4^2 + 2p_3^\mu p_{4\mu}, \quad (17)$$

$$\hat{t} = (p_1 - p_3)^2 = (p_2 - p_4)^2 = m_1^2 + m_3^2 - 2p_1^\mu p_{3\mu} = m_2^2 + m_4^2 - 2p_2^\mu p_{4\mu}, \quad (18)$$

$$\hat{u} = (p_1 - p_4)^2 = (p_2 - p_3)^2 = m_1^2 + m_4^2 - 2p_1^\mu p_{4\mu} = m_2^2 + m_3^2 - 2p_2^\mu p_{3\mu}. \quad (19)$$

In the CM-frame, $\hat{s} = s = (E_1 + E_2)^2$. If, $m_3 = m_4$ and $m_1 = m_2$ with $E_1 = E_2 = E_3 = E_4 = E$, we have

$$t = -(\vec{p}_1 - \vec{p}_3)^2 = -\vec{p}_1^2 - \vec{p}_3^2 + 2\vec{p}_1 \cdot \vec{p}_3 \quad (20)$$

where $\vec{p}_1^2 = E^2 - m_1^2$ and $\vec{p}_3^2 = E^2 - m_3^2$.

So, in terms of s , t could be written as

$$t = -2s + (m_1^2 + m_3^2) + 2\sqrt{(s/4 - m_1^2)(s/4 - m_3^2)} \cos \theta, \quad (21)$$

with θ the scattering angle in the CM-frame.